Selective Formation of Light Olefins from $CO+H_2$ Over Silica Supported Co/CeO_2 Prepared by Fusion Method: Preparation, Characterization and Operational Conditions Effects

A. Beigbabaei[1], A.A. Mirzaei[*,1], M. Galavy[1] and A. Youssefi[2]

[1]*Department of Chemistry, Faculty of Sciences, University of Sistan and Baluchestan, Zahedan 98135-674, Iran*

[2]*Par-e-Taavouse Research Institute, Mashhad, Iran*

Abstract: The catalyst containing 80%Co/20%Ce/15wt%SiO_2 was prepared using fusion procedure and studied for the conversion of synthesis gas to light olefins. The effect of a range of operating variables such as the pressure, temperature and H_2/CO molar feed ratio on the catalytic performance of fused catalyst was investigated. It was found that the best operating conditions are H_2/CO=2/1, T=350˚C and P=2 bar. The results are interpreted in terms of the structure of active catalyst. Characterization of both precursor and calcined catalysts was carried out using Powder X-ray Diffraction (XRD), Scanning Electron Microscopy (SEM) and BET surface area measurements.

Keywords: Co-Ce/SiO_2 catalyst, fusion method, characterization, light olefins, operating conditions.

1. INTRODUCTION

The pressing need to reduce the environmental impact of modern technology and lifestyles imposes the need for continuous development and upgrading of old and novel methodologies aimed at significantly reducing pollutant emissions, mainly from mobile sources, to warrant a tolerable quality of life in large metropolitan areas [1]. This has prompted an extraordinary research effort aimed both at improving emission control system and synthesizing more effective and cleaner fuels from synthesis gas that have lower CO_2, NO_x and SO_x [2-4]. Fischer-Tropsch synthesis (FTS) has attracted increasing attention, since high quality diesel fuels without any sulfur or aromatic compounds can be produced directly from synthesis gas derived from natural gas, coal, or biomass [5]. FTS also provides a means of converting coal and natural gas to petrochemicals and liquid transportation fuels. The FTS product spectrum is very broad and consequently many studies have been carried out under FT conditions with the aim of controlling and limiting the product selectivity. This control is typically achieved by modification of the catalyst, the reactor and/or the reaction conditions [6]. Typically, FTS catalysts include VIII group based metals (Co, Ru, Fe) with Co-based ones ensuring a superior long-chain hydrocarbon yield and longer life time [7-9]. The FT reaction with cobalt-based catalysts has been studied by many researchers [10-15]. An approach to improve the selectivity of classical FT process for conversion of synthesis gas to hydrocarbons involves the use of a bifunctional catalyst system containing a metal catalyst combined with a support. Supported cobalt catalysts are the preferred catalysts for the FT synthesis of long-chain paraffins from synthesis gas made from natural gas. For supported cobalt catalysts, both texture and surface properties of support have a great influence on the dispersion and reducibility of cobalt [16-18]. Numerous studies have been devoted to ascertaining the influence of oxide carriers (e.g. titania, silica, alumina and zirconia) on the activity and stability of Co catalysts [19-24], and have determined that the "site time yield" of Co-based catalysts is not affected by either the degree of dispersion or the support identity [19, 25, 26]. Literature survey has shown that using bimetallic catalysts obtained from alloys may have some special advantages in CO hydrogenation [27,28]. Co-Ce catalysts have been investigated for its selectivity to lower molecular weight olefins [29-31]. The mixed cobalt cerium oxide catalysts supported by SiO_2 [32,33] and TiO_2 [34] have been also tested in FTS for the production of hydrocarbons.

In our previous work [35], we used the co-precipitation method to investigate the effect of a range of precipitation variables such as, precipitate ageing time, the [Co]/[Ce] ratio of the precipitation solution and the catalyst calcination temperatures on the structure of a precipitated cobalt-cerium catalyst in FTS. We also reported further results concerning the effects of different promoters and supports on the catalytic performance of the optimally-prepared catalyst using co-precipitation method [36]. Our works showed that the optimum catalyst has a molar [Co]/[Ce] ratio of 80%Co/20%Ce and is supported by 15wt% SiO_2 based on the total catalyst weight. However, not much systematic work about the other preparation methods of Co/Ce oxide catalysts and their catalytic properties has been reported in the literature. Thus, in continuation of our previous works [35,36], we planed to investigate in outline, the other general preparative methods and characterization of silica supported Co/Ce oxide catalysts and then compare the obtained results with the results of the optimum catalyst made by co-precipitation method to study how preparation method exert

*Address correspondence to this author at the Department of Chemistry, Faculty of Sciences, University of Sistan and Baluchestan, Zahedan 98135-674, Iran; Tel: +98 (541) 2447231; Fax: +98 (541) 2447231;
E-mail: mirzaei@hamoon.usb.ac.ir

1876-214X/10

influence on catalytic activity and selectivity of catalysts in light olefins synthesis from CO and H_2. Now, in this present work, we attempt to extensively report the influence of operating variables such as various H_2/CO molar feed ratios (space velocity) and a range of reaction temperatures and pressures on the catalytic performance of the catalyst containing 80%Co/20%Ce/15wt%SiO_2 which is prepared using fusion method. We also characterized the different catalysts using varying techniques such as Powder X-ray Diffraction (XRD), Scanning Electron Microscopy (SEM) and BET surface area measurement. The effect of all of the operating variables on the catalytic performance of Co-Ce/SiO_2 catalyst prepared by other preparation methods such as sol-gel and impregnation will be reported in future.

2. MATERIALS AND METHODOLOGY

2.1. Catalyst Preparation

In the present study, a catalyst with 80%Co/20%Ce/ 15wt%SiO_2 composition was prepared using fusion method. The required amounts of $Co(NO_3)_2.6H_2O$ and $Ce(NO_3)_3.6H_2O$ and SiO_2 were added to crucible and the mixed materials fused at high temperature. Solid chunks were obtained from the cooled mixture then ground. The catalyst was dried in an oven at 120ºC for 12 h. The dried catalyst was calcined at 600 ºC for 6 h.

2.2. Catalysts Characterization

2.2.1. X-Ray Diffraction (XRD)

Powder XRD measurements were preformed using a D8 Advance diffractometer (Bruker AXS, Germany). Scans were taken with a 2θ step size of 0.02 and a counting time of 1.0 s using a CuK_α radiation source generated at 40 kV and 30 mA. Specimens for XRD were prepared by compaction into a glass-backed aluminum sample holder. Data was collected over a 2θ range from 4˚ to 70˚ and phases were identified by matching experimental patterns to entries in Diffract^{plus} version 6.0 indexing software.

2.2.2. BET Surface Area Measurements

BET surface area measurements were conducted using a surface area analyzer (Nova 2000, Quantachrome Instruments, FL, USA) using nitrogen (99.99% purity) as the adsorption gas. The catalyst samples were slowly heated to 300˚C for 3h under nitrogen atmosphere. To obtain the BET specific surface area measurements, the different precursors and catalysts were evacuated at -196˚C for 66 min.

2.2.3. Scanning Electron Microscopy

The morphology of the catalysts and their precursors was observed by means of a Cambridge S-360 scanning electron microscope (made in England).

2.3. Catalyst Testing

The catalyst tests were carried out in a fixed bed stainless micro reactor operating at atmospheric pressure (Fig. **1**). All gas lines to the reactor bed were made from 1/4" stainless steel tubing. Three mass flow controllers (Brooks, Model 5850E) equipped with a four-channel read out and control equipment (Brooks 0154) were used to adjust automatically the flow rate of the inlet gases (CO, H_2, and N_2 with purity of 99.999%). The mixed gases in the mixing chamber passed into the reactor tube, which was placed inside a tubular furnace (Atbin, Model ATU 150-15) capable of producing temperature up to 1500ºC and controlled by a digital programmable controller (DPC). The reactor tube was constructed from stainless steel tubing; internal diameter of 9 mm, with the catalyst bed situated in the middle of the reactor. The reaction temperature was controlled by a thermocouple inserted into catalyst bed and visually monitored by a computer equipped with software. Some thermocouples inserted in the catalyst bed for monitoring the inlet, outlet and bed temperatures by a DPC. The meshed catalyst (1.0 g) was held in the middle of the reactor with 110 cm length using quartz wool. It consists of an electronic back pressure regulator which can control the total pressure of the desired process using a remote control *via* the TESCOM software package integration that improve or modify its efficiency that capable for working on pressure ranging from atmospheric pressure to 34 bar. The catalyst was pre-reduced in situ atmospheric pressure in a flowing H_2-N_2 stream (N_2/H_2=1, flow rate of each gas=30 ml/min) at 300 ºC for 2h before synthesis gas exposure. The H_2/CO reaction was carried out at 300-450 ºC (P=1 atm, H_2/CO=1.00/4.00, GHSV= 2700-5130 h^{-1}). Reactant and product streams were analyzed on-line using a gas chromatograph (Varian, Model 3400 Series) equipped with a 10-port sampling valve (Supelco company, USA, Visi Model), a sample loop and thermal conductivity detector(TCD). The contents of sample loop were injected automatically into a packed column (Hayesep DB, Altech Company, USA, 1/8" OD, 10 meters long, and particle mesh 100/120). Helium was employed as a carrier gas for optimum sensitivity (flow rate=30 ml/min). The calibration was carried out using various calibration mixtures and pure compounds obtained from American Matheson Gas Company (USA). GC controlling and collection of all chromatograms was done *via* an IF-2000 Single channel data interface (TG Co, Tehran, Iran) at windows® environment. The results in terms of CO conversion, selectivity and yield of products are given at each space velocity. The CO conversion (%) is calculated according to the normalization method:

$$\text{CO conversion } (\%) = \frac{(\text{Moles of CO}_{in}) - (\text{Moles of CO}_{out})}{\text{Moles of CO}_{in}} \times 100$$

The selectivity (%) towards the individual components on carbon-basis is calculated according to the same principle:

$$\text{Selectivity of j product } (\%) = \frac{\text{Moles of j prduct}}{(\text{Moles of CO}_{in}) - (\text{Moles of CO}_{out})} \times 100$$

3. RESULTS AND DISCUSSION

3.1. Effect of Operating Conditions

The operating conditions were investigated to identify and optimize the operation variables, such as H_2/CO molar feed ratios, reaction temperatures and reaction pressures that have a marked effect on the catalytic performance.

3.1.1. Effect of H_2/CO Feed Ratio

The influence of the reaction H_2/CO molar feed ratio on the steady state catalytic performance of the cobalt cerium

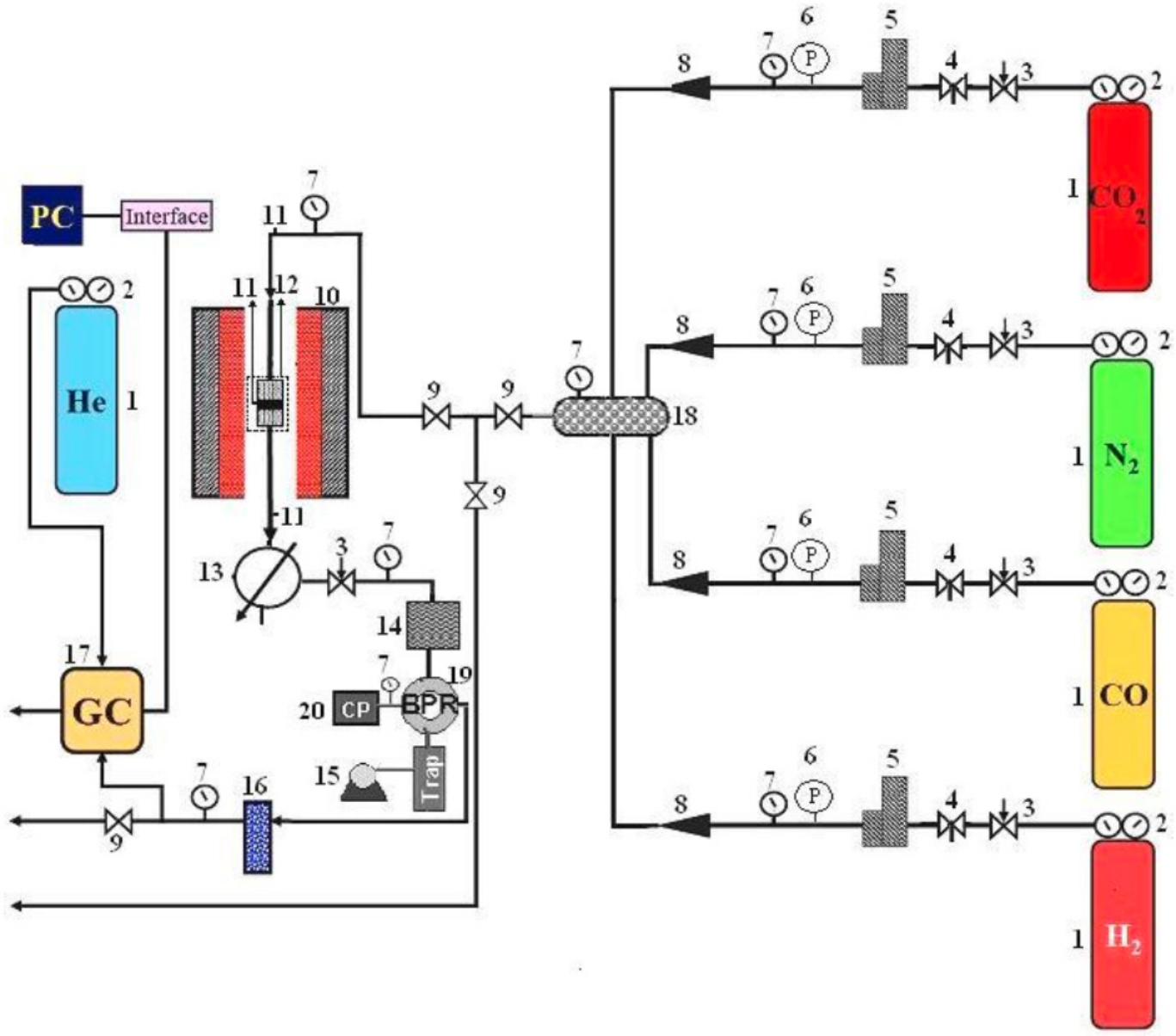

Fig. (1). Schematic representation of the reactor in a flow diagram used. 1-Gas cylinders, 2-Pressure regulators, 3-Needle valves, 4-Valves, 5-Mass Flow Controllers (MFC), 6-Digital pressure controllers, 7-Pressure Gauges, 8-Non return valves, 9-Ball valves, 10-Tubular Furnace, 11-Temperature indicators, 12-Tubular reactor and catalyst bed, 13-Condenser, 14-Trap, 15-Air pump, 16-Silica gel column, 17-Gas Chromatograph (GC), 18-Mixing chamber, 19-BPR: Back Pressure Regulator (Electronically type), 20-CP (Control panel).

oxide catalyst containing 80%Co/20%Ce/15wt%SiO_2 prepared using fusion method for the Fischer-Tropsch reaction at 450˚C under atmospheric pressure was investigated and the results are presented in Fig. (**2**). As it shown in this figure, with variation in H_2/CO feed molar ratios from 1/1 to 4/1, the CO conversion was gradually decreased. It is also apparent that the H_2/CO feed molar ratios from 1/1 to 4/1 gave different selectivities with respect to light olefins. However, as shown on Fig. (**2**), in comparison with the products of the other H_2/CO feed ratios under the same operating conditions of temperature and pressure, it was observed that at a H_2/CO ratio of 2/1, the total selectivity toward C_2-C_4 olefins was higher and the CH_4 selectivity was lower. Taking these results into consideration, the H_2/CO ratio of 2/1 was chosen as the optimum ratio for converting of synthesis gas to C_2-C_4 light olefins using the fused catalyst containing 80%Co/20%Ce/15wt%SiO_2.

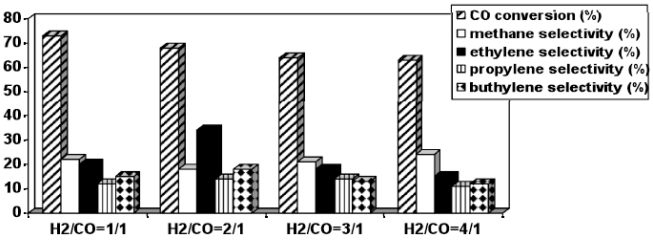

Fig. (2). Effect of different H_2/CO feed ratios on the catalytic performance.

Characterization of this catalyst was carried out using XRD and the patterns of this catalyst in the different stages

of precursor, fresh calcined catalyst (before the test) and used calcined catalyst (after the test) at H_2/CO=2/1 are shown in Fig. (**3**). The catalyst precursor was found to be amorphous; the presence of amorphous phases in the XRD pattern of the precursor makes the other phases undetectable. However, the calcined catalyst before the test showed the different phases and the actual phases identified in this catalyst were $CoSi_2$ (cubic), CeO_2 (cubic), SiO_2, $CeCoSiO_2$(Tetragonal), Co_2SiO_4(Cubic) and Co_3O_4 (cubic). Numerous studies on Co/SiO_2 as a catalyst for the FTS evidence that the calcined catalysts have the phase composition of Co_3O_4 + SiO_2, exhibiting no interaction of the metal oxide with the silica support occurred [37-41]. In order to identify the changes in calcined catalyst during the reaction and to detect the phases formed, the catalyst after the test was characterized by XRD and its phases were found to be $CoSi_2$ (cubic), CeO_2 (cubic), CoO (cubic), C (hexagonal), Co_2C (orthorhombic), Ce (cubic), Co (hexagonal) and Ce_2C_3 (cubic). During chemical reaction, some of the oxidic phases in calcined catalyst before the test transform into the metallic and carbide phases; and so in the tested catalyst, there are oxidic and carbide phases which both of them are active phases in the FTS. Carbide phase is active in CO hydrogenation. Formation of this phase with oxidic phases which are active to olefins cause high performance of supported SiO_2 catalyst [42,43]. Clearly, the XRD study suggests that the precursor undergoes a morphological changing during calcination and also FTS chemical reaction. However, the XRD technique may not be sufficiently sensitive to follow the fine details of these changes. In view of this, a detailed SEM study of the precursor and calcined catalysts before and after the test at optimum molar feed ratio of 2/1 was undertaken and their SEM images on different stages are presented in Fig. (**4**). The SEM observations showed differences in morphology of precursor and calcined catalysts (before and after the test). The electron micrograph obtained from the catalyst precursor (Fig. **4a**) was found to be composed of several agglomerates of irregularly-spherical shaped grains and shows that this material has a high dense and homogeneous morphology. After the calcination at 600˚C, the morphological features were different to the precursor sample and showed that the agglomerate measure was greatly reduced compared with the precursor. The SEM image of the calcined catalyst before the test revealed that this catalyst comprised of small grains which are adhesived to the voluminous bulks (Fig. **4b**). After FTS chemical reaction the catalyst texture and its morphology changed (Fig. **4c**). However, the size of the grains in the tested catalyst grew larger by agglomeration, which may be due to sintering after reactions. This is consistent with previous study by Galarrage *et al.* [44], who observed that temperature could cause agglomeration of these small grains, which correlates with catalyst deactivation under high temperature. The diffraction pattern of the catalyst before the test showed that different phases of the precursor transform into the oxidic phases. The diffraction pattern of the catalyst after the test showed that the oxidic phases in calcined catalyst transform into the metallic and carbide phases. It therefore appears that these phases enhance agglomerate size growth as shown by the SEM image of the catalyst after the test (Fig. **4c**).

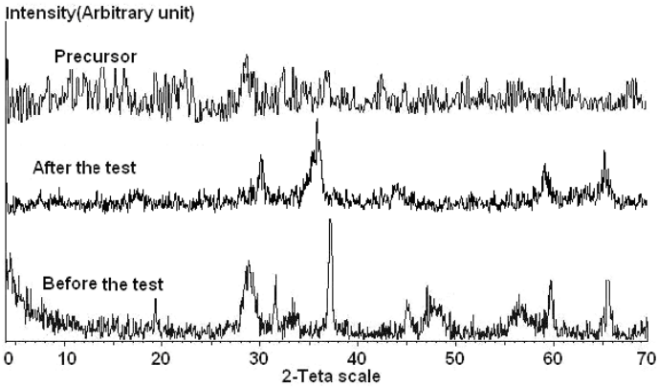

Fig. (3). XRD patterns of precursor and calcined catalysts (before and after the test) containing 80%Co/20%Ce/15wt% SiO_2.

3.1.2. Effect of Reaction Temperature

The effect of reaction temperature, ranging from 300-450ºC on the catalytic performance of the 80%Co/20%Ce/15wt%SiO_2 prepared using fusion method, was studied (P=1atm, H_2/CO=2/1 and GHSV=4500h^{-1}). According to the obtained results (Fig. **5**), the optimum reaction temperature was 350 ºC, temperature at which the total selectivity of light olefins products was higher than

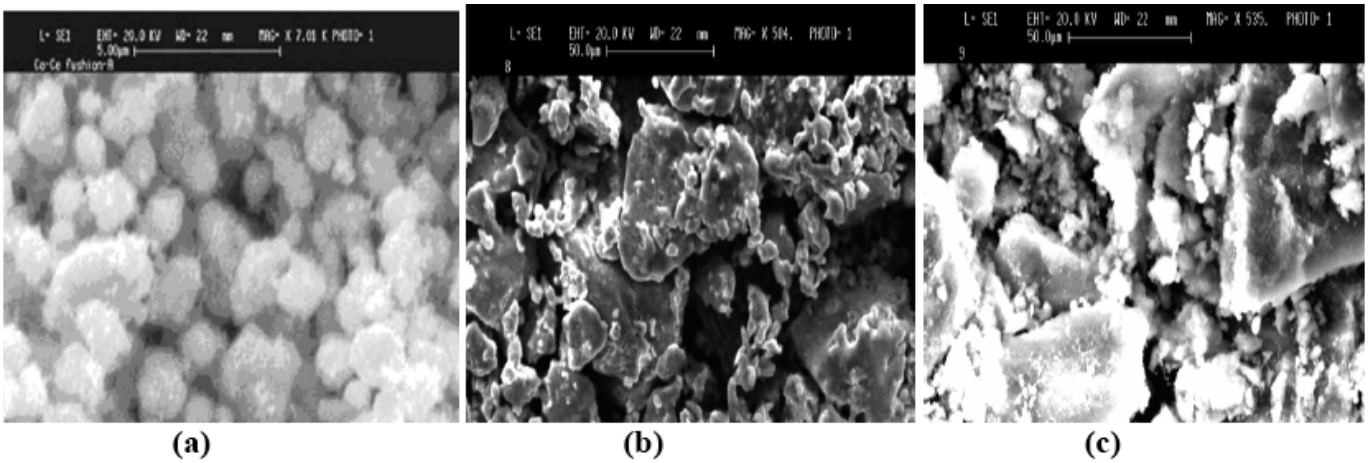

Fig. (4). SEM images of 80%Co/20%Ce/15wt% SiO_2 catalyst in (**a**) precursor (**b**) catalyst before the test (**c**) catalyst after the test at H_2/CO=2/1.

those at the other reaction temperatures under the same operating conditions. Also, the CO conversion was high, CH_4 selectivity was low and no coke was formed at 350˚C. In general, an increase in the reaction temperature leads to an increase in the catalytic performance, however, it was also shown that the reactor temperature should not be too low since in the low reaction temperatures, the conversion percentage of CO is low, giving a high level of methane production [45]. On the other hand, an increase in the reaction temperature leads to the formation of large amounts of coke as an unwanted by-product; as we found in this work. All of the catalysts after the test at different temperatures were characterized using XRD method and their patterns are presented in Fig. (**6**). As it shown, all of them have the same phases including $CoSi_2$ (cubic), CeO_2 (cubic), CoO (cubic), C (hexagonal), Co_2C (orthorhombic), Ce (cubic), Co (hexagonal) and Ce_2C_3 (cubic). To obtain a better understanding from the structure changes of the catalyst during reaction temperature changes, the morphology of the catalyst after the test at the optimal reaction temperature of 350˚C was studied using SEM method and the SEM image of this catalyst (Fig. **7a**) that compared with the SEM image of the catalyst tested at the maximum reaction temperature of 450˚C (Fig. **7b**) are presented in Fig. (**7**). As shown, the morphology and texture of these catalysts are quite different. The catalyst tested at 450˚C has a more adhesive texture and also has rough and disproportionate agglomerate; this may be due to sintering after the test at this temperature. Whereas the catalyst tested at 350˚C has a more homogeneous and less sticky texture. It can be concluded that the sintering phenomenon occurs less at lower temperature; this may be a reason why the catalyst tested at 350˚C showed the best catalytic performance. It should be mentioned here that the catalyst tested at 450˚C was found to be mixed with coke; this can be also resulting to sintering at this temperature.

3.1.3. Effect of Total Reaction Pressure

An increase in total pressure would generally result in condensation of hydrocarbons, which are normally in the gaseous state at atmospheric pressure. High pressures and higher carbon monoxide conversions would probably lead to saturation of catalyst pores by liquid reaction products [46].

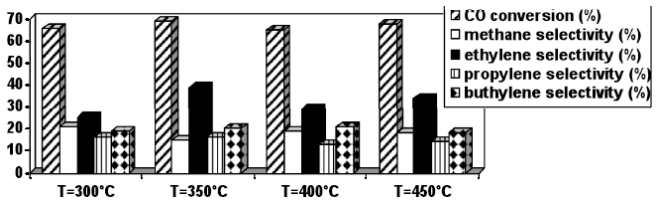

Fig. (5). Effect of different reaction temperatures on the catalytic performance.

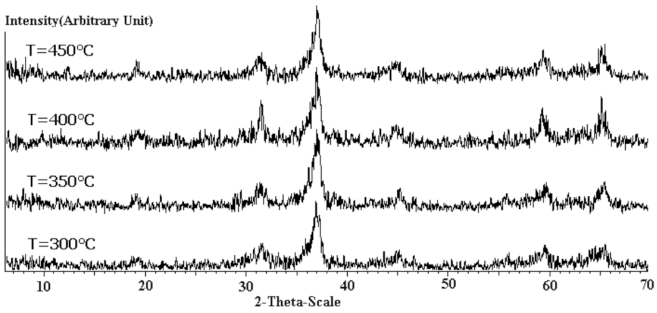

Fig. (6). XRD patterns of the 80%Co/20%Ce/15wt%SiO_2 catalyst after the test at different reaction temperatures.

A different composition of the liquid phase in catalyst pores at high syngas pressures could affect the rate of elementary steps and carbon monoxide and hydrocarbon concentrations. The influence of the reaction pressure on the catalytic performance of the fused cobalt cerium oxide catalyst containing 80%Co/20%Ce/15wt.%SiO_2 for production of light olefins at 350 ºC and H_2/CO=2/1 was investigated and the results are presented in Fig. (**8**). The results indicate that at the total pressure of 1 bar, the optimal catalyst showed a total selectivity of 75% with respect to C_2-C_4 light olefins and did not produce the C_5^+ products. It is also apparent that increasing in total pressure in the ranges of 2-10 bar significantly increases the C_5^+ selectivity. In the other hand, as it can be seen on Fig. (**8**), with the exception of 2 bar total pressure, at the ranges of 1-10 bar total pressure, no significant change on CO conversion was observed, however, the light olefins selectivities were changed and the results indicate that at the total pressure of 2 bar, the fused catalyst containing 80%Co/20%Ce/15wt%.SiO_2 showed the highest total selectivity of 82% with respect to C_2-C_4 light

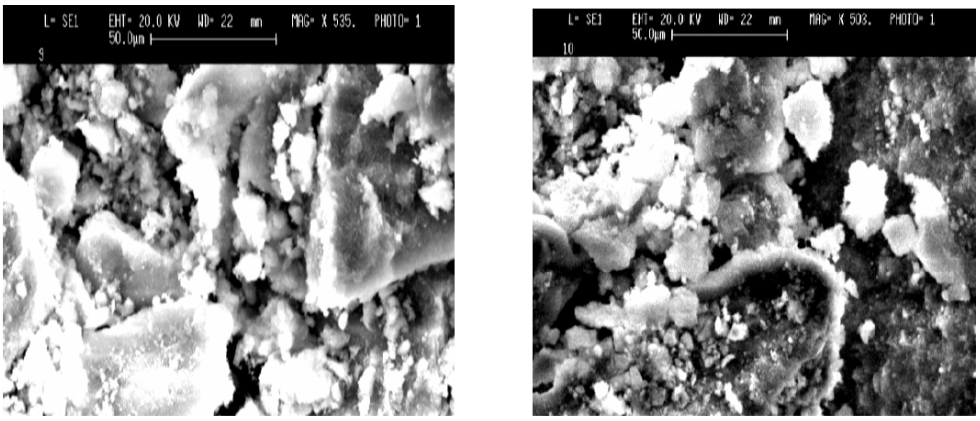

Fig. (7). SEM images of the catalyst after the test at (**a**) T=350˚C (**b**) T=450˚C.

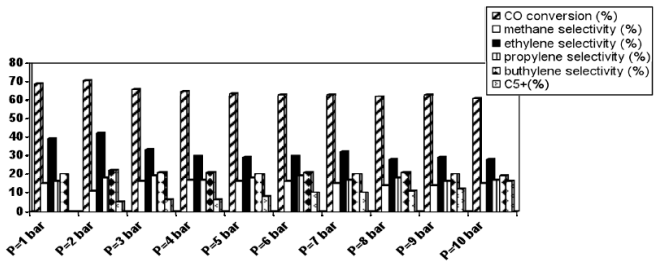

Fig. (8). Effect of different reaction pressures on the catalytic performance.

olefins. Hence, because of high CO conversion, low CH_4 selectivity and also higher total selectivity with respect to C_2-C_4 light olefins at the total pressure of 2 bar, this pressure was chosen as the optimum pressure. All of these catalysts after the test at different pressures were characterized using XRD method and their XRD patterns are presented on Fig. (**9**). As shown, all of these tested catalysts have the same phases including $CoSi_2$ (cubic), CeO_2 (cubic), CoO (cubic), C (hexagonal), Co_2C (orthorhombic), Ce (cubic), Co (hexagonal) and Ce_2C_3 (cubic); the oxidic and carbide phases are active in Fischer-Tropsch synthesis for conversion of synthesis gas to olefins. The morphology of the catalyst tested at pressure of 2 bar was investigated using scanning electron microscopy technique and the SEM image of this catalyst that compared with the SEM image of the catalyst tested at pressure of 1 bar, are presented in Fig. (**10**). These images revealed that the morphology of the catalyst is clearly depends on the reaction pressure and the catalyst tested at pressure of 2 bar has a different morphology and texture with the catalyst tested at pressure of 1 bar. The catalyst tested at pressure of 1 bar has a non-uniform agglomerate and also has a more sticky texture; this catalyst comprise of particles with different size (10a). Whereas the catalyst tested at pressure of 2 bar has a more homogeneous texture and high dense agglomerate of particles; in this catalyst the particle size of some grains slightly increased (10b). The BET surface area measurement was used in order to measure the specific surface area of catalyst. The specific surface area of the catalyst tested at pressure of 2 bar that compared with the precursor and calcined catalyst before the test are presented in Table **1**. As shown, the calcined catalyst before the test has a higher specific surface area (119 m^2/g) than its precursor (103 m^2/g); this is in agreement with the SEM results which showed that the agglomerate size of calcined catalyst is less than of its precursor and therefore leads to an increase in the BET specific surface area of the calcined sample. The high specific surface area of calcined catalyst before the test allows a high degree of metal dispersion.

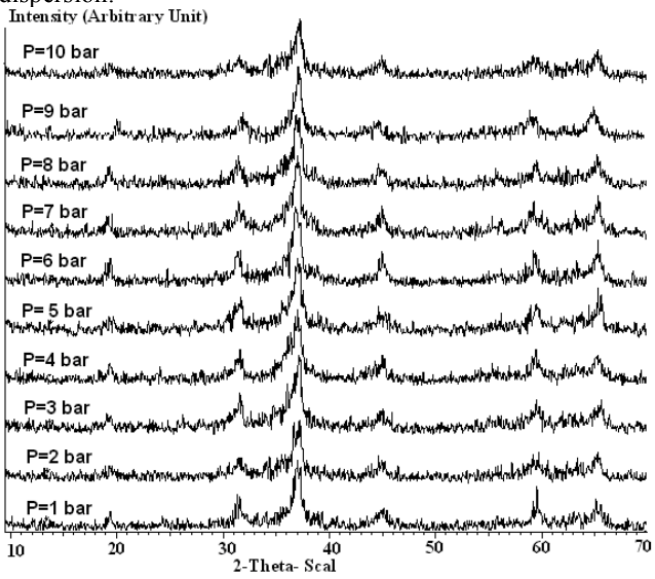

Fig. (9). XRD patterns of the 80%Co/20%Ce/15wt%SiO_2 catalyst after the test at different reaction pressures.

4. CONCLUSION

The Co-Ce/SiO_2 catalyst which has been prepared using fusion procedure was tested at different reaction conditions and it was found that the operating conditions have a great effect on the structure and catalytic performance of the catalyst. The effect of variable factors such as reaction temperature, reaction pressure and H_2/CO molar feed ratios were examined on the catalytic performance of the fused catalyst containing 80%Co/20%Ce/15wt%SiO_2. The optimal operating conditions for production highest selectivity toward light olefins were found to be 350˚C with molar feed ratio of H_2/CO=2/1 under the total pressure of 2 bar. The

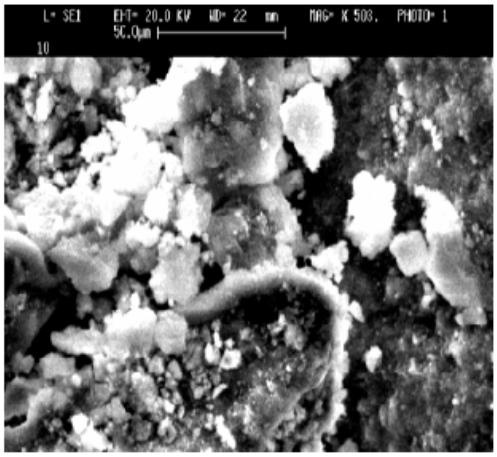

(a) P=1 bar

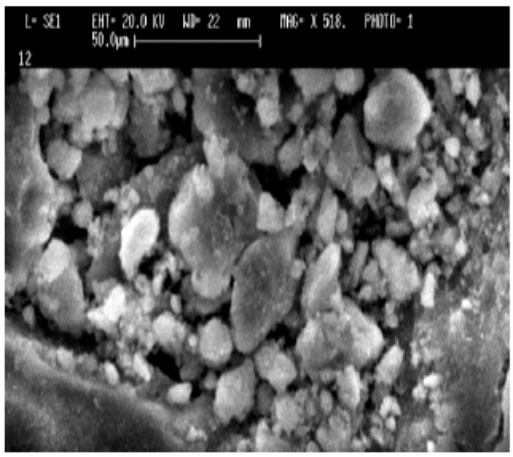

(b) P=2 bar

Fig. (10). SEM images of the catalyst after the test at (**a**) P=1bar (**b**) P=2 bar.

characterization of precursor and calcined catalysts (before and after the test) was performed by powder XRD, SEM and BET surface area measurement. These results showed that the catalyst is sensitive to the operating conditions. These operating parameters should be incorporated to achieve the highest selectivity toward light olefins from the catalyst containing 80%Co/20%Ce/15wt%SiO_2 prepared using fusion procedure.

Table 1. BET Results of the Catalyst Containing 80%Co-20%Ce/15wt%SiO_2

Fused Catalyst	Specific Surface Area (m^2/g)		
	Precursor	Fresh Catalyst	Used Catalyst
80%Co/20%Ce/15wt%SiO_2	103	119	115

REFERENCES

[1] Spadaro, L.; Arena, F.; Granados, M. L.; Ojeda, M.; G. Fierro.; Frusteri, F. Metal–support interactions and reactivity of Co/CeO_2 catalysts in the Fischer–Tropsch synthesis reaction. *J. Catal.,* **2005**, *234*, 451-462.

[2] Shen. J.; Schmetz. E.; Kawalkin. G. J.; Winslow. J. C.; Noceti. R. P.; Nowak. M. A.; Krastman. D.; Tomer. B. J.; Symposium on Advances in Fischer-Tropsch Chemistry, 219th National Meeting, ACS, San Francisco, **2000**.

[3] Schulz, H. Preface. *Top. Catal*, **2003**, *26*, 1-2.

[4] Fleisch, H.; Sills, R. A. Large-scale gas conversion through oxygenates: beyond GTL-FT. *Stud. Surf. Sci. Catal.,* **2004**, *147*, 31-34.

[5] Li, X.; Luo, M.; Asami, K. Direct synthesis of middle iso-paraffins from synthesis gas on hybrid catalysts. *Catal. Today*, **2004**, *89*, 439-446.

[6] Schulz, H. Short history and present trends of Fischer–Tropsch synthesis. *Appl. Catal. A Gen.*, **1999**, *186*, 3-12.

[7] Van Berge, P. J.; Everson. R. C. Cobalt as an alternative Fischer-Tropsch catalyst to iron for the production of middle distillates. *Stud. Surf. Sci. Catal.,* **1997**, *107*, 207-212.

[8] Van der Laan, G. P.; Beenackers, A. A. C. M. Kinetics and selectivity of the fischer-tropsch synthesis: A literature review. *Catal. Rev. Sci. Eng.,* **1999**, *41*, 255-318.

[9] Chaumette, P.; Coutry, Ph.; Kiennemann, A.; Ernst, B. Higher alcohol and paraffin synthesis on cobalt based catalysts: comparison of mechanistic aspects. *Top. Catal.,* **1995**, *2*, 117-126.

[10] Yang, C. H.; Massoth, F. E.; Oblad, A. G. Kinetics of CO + H_2 reaction over co-Cu-Al_2O_3 catalyst. *Adv. Chem. Ser.,* **1979**, *178*, 35-46.

[11] Rautavoma, A. O.; Van der Baan, H. S. Kinetics and mechanism of the Fischer- Tropsch hydrocarbon synthesis on a cobalt on alumina catalyst. *Appl. Catal. A Gen.,* **1981**, *1*, 247-272.

[12] Sarup, B.; Wojciechowski, B. W. Studies of the fischer-tropsch synthesis on a colbalt catalyst. III. mechanistic formulation of the kinetics of selectivity for higher hydrocarbon formation. *Can. J. Chem. Eng.,* **1989**, *67*, 620-627.

[13] Yates, I. C.; Satterfield, C. N. Intrinsic kinetics of the fischer-tropsch synthesis on a cobalt catalyst. *Energy Fuel.,* **1991**, *5*, 168-173.

[14] Iglesia, E.; Reyes, S. C.; Madon, J. R.; Soled, S. I. Selectivity control and catalyst design in the fischer-tropsch synthesis: sites, pellets, and reactors. *Adv. Catal. Relat. Subj.,* **1993**, *39*, 221-302.

[15] Chanenchuk, C. A.; Yates, I. C.; Satterfield, C. N. The fischer-tropsch synthesis with a mechanical mixture of a cobalt catalyst and a copper-based water gas shift catalyst. *Energy Fuel.,* **1991**, *5*, 847-855.

[16] Dimitrova, P. G.; Mehandjiev, D. R. Active surface of γ-Al_2O_3-supported Co_3O_4. *J. Catal.,* **1994**, *145*, 356-363.

[17] Bessell, B. Support effects in cobalt-based fischer-tropsch catalysis. *Appl. Catal. A Gen.,* **1993**, *96*, 253-268.

[18] Lapszewicz, J. A.; Loeh, H. J.; Chipperfield, J. R. The effect of catalyst porosity on methane selectivity in the fischer–tropsch reaction. *J. Chem. Soc. Chem. Commun.,* **1993**, *11*, 913-914.

[19] Iglesia, E. Design, synthesis, and use of cobalt-based fischer-tropsch synthesis catalysts. *Appl. Catal. A Gen* **1997**, *161*, 59-78.

[20] Adachi, M.; Yoshii, K.; Han, Y. Z.; Fugimoto, K. Fischer–tropsch synthesis with supported cobalt catalyst. promoting effects of lanthanum oxide for cobalt/silica. *Catal. Bull. Chem. Soc. Jap.,* **1996**, *69*, 1509-1516.

[21] Kogellbauer, A.; Goodwin, J. G.; Oukaci, R. Ruthenium promotion of Co/Al_2O_3 fischer–tropsch catalysts. *J. Catal.,* **1996**, *160*, 125-133.

[22] Hurlbut, R. S.; Puskas, I.; Schumacher, D. J. Fine details on the selectivity and kinetics of the fischer−tropsch synthesis over cobalt catalysts by combination of quantitative gas chromatography and modeling. *Energy Fuel.,* **1996**, *10*, 537-545.

[23] Van de Loosdrecht, J.; Van der Harr, M.; Van der Kraan, A. M.; Van Dillen, A. J.; Geus, J. W. Preparation and properties of supported cobalt catalysts for fischer-tropsch synthesis. *Appl. Catal. A Gen.,* **1997**, *150*, 365-376.

[24] Matsuzaki, T.; Takeuchi, K.; Hanaoka, T.; Arakawa, H.; Sugi, Y.; Wei, K. M.; Dong, T. L.; Reinikainen, M. Oxygenates from syngas over highly dispersed cobalt catalysts. *Catal. Today,* **1997**, *36*, 311-324.

[25] Iglesia, E.; Soled, S. L.; Fiato, R. A. Fischer-tropsch synthesis on cobalt and ruthenium. metal dispersion and support effects on reaction rate and selectivity. *J. Catal.,* **1992**, *137*, 212-224.

[26] Iglesia, E.; Soled, S. L.; Baumgartner, J. E.; Reyest, S. C. Synthesis and catalytic properties of eggshell cobalt catalysts for the fischer-tropsch synthesis. *J. Catal.,* **1995**, *153*, 108-122.

[27] Stoop, F.; Wiele, K. V. Formation of olefins from synthesis gas over silica-supported RuFe bimetallic catalysts. *Appl. Catal. A Gen.,* **1986**, *23*, 35-47.

[28] Arakawa, H.; Kiyozumi, Y.; Suzuki, K.; Takeuchi, K.; Matsuzaki, T.; Sugi, Y.; Fukushima, T.; Matsushita, S. Selective synthesis of ethylene from synthesis gas over hybrid catalyst system. *Chem. Lett.,* **1986**, *15*, 1341-1342.

[29] Bruce, L.A.; Hoong, M.; Hughes, A.E.; Turney, T.W. In: Curru-Hyde. H. E Howe. R. F.; Eds. *Natural Gas Conversion II,* Elsevier Science, **1994**, pp. 427-432.

[30] Barault, J.; Guilleminot, A.; Achard, J. C.; Paul-Boneour, V.; Percheron Guegan, A.; Hilaire, L.; Coulon, M. Syngas reaction over lanthanum-cobalt intermetallic catalysts. *Appl. Catal. A Gen.,* **1986**, *22*, 273-287.

[31] Bruce, L. A.; Hoang, M.; Hughes, A. E.; Turney, T. W. Ruthenium promotion of Fischer-Tropsch synthesis over coprecipitated cobalt/ceria catalysts. *Appl. Catal. A Gen* **1993**, *100*, 51-67.

[32] Dai, X.; Yu, C.; Li, R.; Shi, H.; Shen, S. Role of CeO_2 Promoter in Co/SiO_2 Catalyst for Fischer-Tropsch Synthesis. *Chin. J. Catal.,* **2006**, *27*, 904-910.

[33] Ernst, B.; Hilaire, L.; Kiennemann, A. Effects of highly dispersed ceria addition on reducibility, activity and hydrocarbon chain growth of a Co/SiO_2 Fischer–Tropsch catalyst. *Catal. Today,* **1999**, *50*, 413-427.

[34] Dai, X.; Yu, C.; Shen, S. Promotion effect of ceria on Fischer – Tropsch synthesis performance over Co/Al_2O_3 catalyst. *Chin. J. Catal.,* **2001**, *22*, 104-108.

[35] Mirzaei, A. A.; Galavy, M.; Beigbabaei, A.; Eslamimanesh, V. Preparation and operating conditions for cobalt cerium oxide catalysts used in the conversion of synthesis gas into light olefins. *J. Iran. Chem. Soc.,* **2007**, *4*, 347-363.

[36] Mirzaei, A. A.; Galavy, M.; Eslamimanesh, V. SEM and BET Methods for investigating the structure and morphology of Co–Ce catalysts for production of light olefins. *Aust. J. Chem.,* **2008**, *61*, 144-152.

[37] Khassin, A. A.; Yurieva, T. M.; Kustova, G. N.; Plyasova, L. M.; Itenberg, I. Sh.; Demeshkina, M. P.; Chermashentseva, G. K.; Anufrienko, V. F.; Zaikovskii, V. I.; Larina, T. V.; Molina, I. Y.; Parmon, V. N. Cobalt-containing catalysts supported by synthetic Zn- and Mg-stevensites and their performance in the fischer–tropsch synthesis. *J. Mol. Catal. A Chem.,* **2001**, *168*, 209-224.

[38] Castner, D. G.; Watson, P. R.; Chan, I. Y. X-ray absorption spectroscopy, X-ray photoelectron spectroscopy, and analytical electron microscopy studies of cobalt catalysts. 1. Characterization of calcined catalysts. *J. Phys. Chem.,* **1989**, *93*, 3188-3194.

[39] Lapidus, A.; Krylova, A.; Kazanskii, V.; Borovikov, V.; Zaitsev, A.; Rathousky, J.; Zukai, A.; Jancalkova, M. Hydrocarbon synthesis from carbon monoxide and hydrogen on impregnated cobalt catalysts Part I. Physico-chemical properties of 10%

cobalt/alumina and 10% cobalt/silica. *Appl. Catal. A Gen.,* **1991**, *73*, 65-81.

[40] Okamoto, Y.; Nagata, K.; Adachi, T.; Imanaka, T.; Inamura, K.; Takyu, T. Preparation and characterization of highly dispersed cobalt oxide and sulfide catalysts supported on silica. *J. Phys. Chem.,* **1991**, *95*, 310-319.

[41] Ming, H.; Baker, B. G. Characterization of cobalt fischer-tropsch catalysts I. unpromoted cobalt-silica gel catalysts. *Appl. Catal. A Gen.,* **1995**, *123*, 23-36.

[42] Zhang, H. B.; Schrader, G. L. Characterization of a fused iron catalyst for fischer-tropsch synthesis by *in situ* laser raman spectroscopy. *J. Catal.,* **1985**, *95*, 325-332.

[43] Shroff, M. D.; Kalakkad, D. S.; Coulter, K. E.; Kohler, S. D.; Harrington, M. S.; Jackson, N. B.; Sault, A. G.; Datye, A. K. activation of precipitated iron fischer-tropsch synthesis catalysts. *J. Catal.,* **1995**, *156*, 185-207.

[44] Galarrage, C. E, Heterogeneous catalyst for the synthesis of middle distillate hydrocarbons. M. S. Thesis, University of Western Qntario, London, **1998**.

[45] Barrault, J.; Forquy, C.; Perrichon, V. Effects of manganese oxide and sulphate on olefin selectivity of iron supported catalysts in the Fischer-Tropsch reaction. *Appl. Catal. A Gen.,* **1983**, *5*, 119-125.

[46] Gribval-Constant, A.; Khodakov, A. Y.; Bechara, R.; Zholobenko, V. L. Support mesoporosity: a tool for better control of catalytic behavior of cobalt supported fischer-tropsch catalysts. *Stud. Surf. Sci. Catal.,* **2002**, *144*, 609-616.

Received: October 27, 2009 Revised: December 18, 2009 Accepted: January 1, 2010